Science of the Total Environment 654 (2019) 616–632

Contents lists available at ScienceDirect

Science of the Total Environment

journal homepage: www.elsevier.com/locate/scitotenv

Optimal irrigation planning for addressing current or future water scarcity in Mediterranean tree crops

Nektarios N. Kourgialas [a,*], Georgios C. Koubouris [b], Zoi Dokou [c]

[a] NAGREF - Hellenic Agricultural Organization (H.A.O.-DEMETER), Institute for Olive Tree Subtropical Crops and Viticulture, Water Recourses-Irrigation & Env. Geoinformatics Lab., Chania, Greece
[b] NAGREF - Hellenic Agricultural Organization (H.A.O.-DEMETER), Institute for Olive Tree Subtropical Crops and Viticulture, Olive Cultivation Lab., Chania, Greece
[c] Department of Civil and Environmental Engineering, University of Connecticut, Storrs, CT, United States

HIGHLIGHTS

- A new decision-making tool for agricultural water management is introduced
- Field measurements and modeling tools were used to predict pore water pressure variations
- Guidance tools for cost-effective irrigation based on pressure thresholds were developed
- Water use can be reduced by up to 41% compared to conventional irrigation practices
- The highest water savings are observed for scenario RCP 4.5 during the studied period

GRAPHICAL ABSTRACT

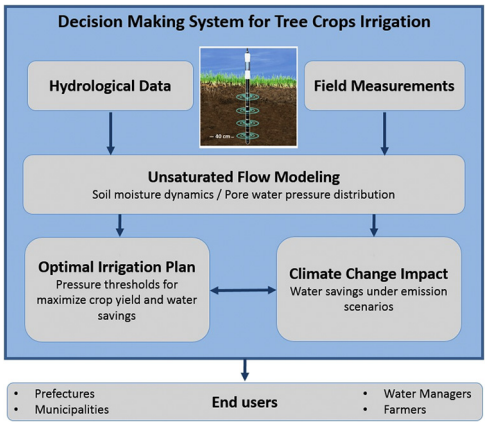

ARTICLE INFO

Article history:
Received 13 September 2018
Received in revised form 6 November 2018
Accepted 8 November 2018
Available online 9 November 2018

Editor: Damia Barcelo

Keywords:
Agricultural water management
Climate change
Cost-effective irrigation plan
Crete
Olive and citrus cultivations
Unsaturated zone

ABSTRACT

Water scarcity in the Mediterranean region is becoming a growing concern, threatening the viability of agriculture, which is one of the main economic sectors in many areas. The design of an optimal irrigation management plan, based on state-of-the-art measuring and modeling tools, can effectively contribute towards water saving efforts and potentially address the water scarcity issue in the region. This paper describes the development and application of an integrated decision-making system for the management of water resources of olive and citrus crops in the North of Chania, Crete, Greece. The system integrates different field measurements, for example 2088 soil moisture measurements taken within the study area, and modeling approaches to simulate flow in the unsaturated zone. After the successful calibration and validation of the model, the spatio-temporal representation of soil moisture and pore water pressure were used as guidance for developing optimal irrigation plans, taking into account the water needs of olive and citrus crops, aiming to maximize crop yield, agricultural income, and promote water saving efforts. According to the results, water use can be reduced by up to 36% during the dry season, compared to conventional irrigation practices for citrus trees. Similarly, for olive trees, the reduction in water use can reach up to 41%. The proposed methodology can also be cost-effective in terms of water value, saving about 40% from the typical water cost for irrigation in the study area. The impact of climate change on water resources availability in the area and water conservation efforts were also investigated for the period of

* Corresponding author.
E-mail address: kourgialas@nagref-cha.gr (N.N. Kourgialas).

https://doi.org/10.1016/j.scitotenv.2018.11.118

(2019–2030). Results show that, comparing the Baseline, RCP 8.5 and RCP 4.5 climatic scenarios, the highest savings on average are observed for emission scenario RCP 4.5 with 53.3% water savings for olive trees and 46.7% for citrus trees.

1. Introduction

The unsaturated soil zone is considered as one of the most critical zones, determining the availability of water through the dynamic balance between precipitation, infiltration and evapotranspiration. Knowledge of the hydraulic properties of the soil is particularly important for understanding the flow and soil moisture content in the unsaturated zone which in turn affects plant growth and crop yields. In addition, understanding the natural processes affecting flow in the unsaturated zone is crucial for designing optimal irrigation plans and for maintaining soil moisture at desirable levels, ensuring satisfactory agricultural production (Šimůnek and Nimmo, 2005). However, the complexity in the composition of the unsaturated zone (coexistence of soil, water, air, plant tissue and microorganisms) makes the study of the relevant hydrological processes a particularly difficult task. As a result, using scientific knowledge to provide practical recommendations on the optimal management of water resources in agriculture remains a challenge.

The unsaturated zone is typically heterogeneous and characterized by temporal variations in soil moisture, which may be replenished by rainfall or removed by evapotranspiration and recharge of the underlying aquifer. The quantification of water losses under the root system zone is a very difficult task because of the uncertainties associated with the flow estimates during the recharge process. In addition, the collection of field measurements to determine soil moisture in relation to soil depth both spatially and temporally is a laborious, time-consuming and costly process (Phogat et al., 2013). A solution to this problem is provided by simulation models that have proved to be particularly useful tools for quantifying and forecasting water potential and irrigation needs in large agricultural areas where experimental procedures are costly and time-consuming (Twarakavi et al., 2010).

In this context, there are three different modeling approaches for simulating flow and soil moisture in the unsaturated zone (DHI, 2011): a) 3D models that solve Richards equation, requiring relationships between the characteristic soil-water curves, b) simplified 1D models of gravity-based flow, which assume a single vertical slope, ignoring capillary forces, and c) simple water balance models or tipping bucket models, which are typically applied to shallow aquifers. In the present study, in order to accurately simulate the flow in the unsaturated zone, the first method was used and implemented using the three-dimensional, finite difference model MIKE SHE.

Designing a proper irrigation plan with water conservation in mind, is one of the primary concerns of modern agriculture. This is very relevant for the island of Crete, given the fact that the major water use is for irrigation purposes (84.5% of the total consumption) (Chartzoulakis et al., 2001). Previous work by Udias et al. (2018) used, at watershed scale, a decision support tool incorporating the SWAT model and sustainable agricultural scenarios to identify irrigation strategies for the island of Crete. For designing an efficient irrigation plan for tree crops, the main factors to be considered are the water requirement of the crops, the timing of irrigation, and the irrigation method. Currently, in Crete, low-volume drip and micro-sprinkler irrigation systems have become the standard irrigation methods for tree crops (Chartzoulakis et al., 2001). However, regardless of the type of irrigation method used, it is necessary to develop an optimal irrigation scheme to supply water at the “right” time and in the “right” amount and rate to avoid excess runoff, water logging or percolation to depths below the root zone. Irrigation scheduling in most cases is based on analysis of common meteorological parameters and crop coefficients. Recent developments in the field of wireless sensor technology have led to the adoption of precision agriculture (PA) which allows agronomists to use sensor - collected soil moisture data to effectively design an irrigation plan. For example, Goldstein et al. (2017) used data collected for a period of 2 years from 22 soil moisture sensors spread in four major plots in a Jojoba orchard in Israel to propose a weekly irrigation plan, using various regression and classification algorithms. Tan et al. (2017) used a multi-objective fuzzy–robust programming (MOFRP) method for supporting the optimal use of land and water resources in agriculture, taking ecological services of crop cultivation into account and applied this method in arid north-western China.

The crop water needs are strongly affected by climatic change, which has been becoming more and more intense in the Mediterranean region (Milano et al., 2013; Nguyen et al., 2016). On a global scale, these changes are captured by Global Climate Models (GCMs) that are used to predict future climatic conditions. The spatial resolution of today's GCMs is of the order of hundreds of km and it is considered low for running environmental impact models that require resolution at <10 km. In this case, a downscaling methodology is needed in order to use the GCM estimates in smaller catchment areas. Two main scale-reduction techniques are the most frequently used; a dynamic approach using Regional-scale Models (RCM) or a statistical approach (Vasiliades et al., 2009; Sapriza-Azuri et al., 2015). Compared to RCMs, statistical methods include simpler computational processes, as well as the ability to produce results that can be compared directly with local observations (Bardossy et al., 2005; Haylock et al., 2006). Therefore, statistical scale-reduction techniques have been preferably used for climate change studies (Varis et al., 2004; Xu et al., 2005; Loukas et al., 2008; Vasiliades et al., 2009; Kourgialas et al., 2015; Gupta et al., 2016) and are also used in this study.

Based on the analysis of meteorological data by Tsanis et al. (2011) for the island of Crete, three different global climatic models GCMs (ECHAM5, IPSL, and CNRM) and two emission scenarios (RCP 8.5 and RCP 4.5) with a spatial resolution of 0.5° were used in this study. For climatic applications, in order to reduce the uncertainties in emission scenarios, multi-regional climate models were found to perform better than predictions from the implementation of only one model (Tebaldi and Knutti, 2007).

The main objective of this research is the development of an integrated decision-making system for the management of water resources in olive and citrus crops in the North of Chania (covering an area of about 215 km^2). This work uses a catchment scale, high resolution (computational cell 20 × 20 m) modeling tool to predict soil moisture and pore water pressure variations in the unsaturated zone. Due to the high model resolution, the results are produced at scales relevant to the farmers. This work introduces an innovative way to establish an optimal irrigation plan, which integrates experimental knowledge on the effect of pore water pressure on the expected yield of citrus and olive trees with a calibrated and validated numerical model, through the use of a pressure threshold approach for maximizing agricultural income and water savings. The impact of climate change on water resources availability in the area was also investigated to assess how scientifically-driven water conservation efforts can be applied in a climate changing environment. This decision making tool can be transferred to the appropriate stakeholders and water managers to improve their ability to provide farmers with optimal irrigation plans that will ensure the sustainability of the agricultural sector under water scarcity conditions.

2. Methodology

2.1. Decision making system

The proposed decision making system comprises of the following components: 1) Collection of available meteorological, land use and groundwater level data, 2) Collection of in-situ field measurements of soil moisture, soil composition and Leaf Area Index (LAI) parameters, 3) Simulation of flow in the unsaturated zone to obtain soil moisture and pore water pressure distribution, 4) Design of an optimal irrigation plan (irrigation onset, frequency and application rate) using pressure as guidance (threshold methodology), 5) Assessment of the impact of climate change on the optimal irrigation plan and potential water savings (Fig. 1). All the data used in the decision making system underwent quality control to ensure data integrity, correctness, and completeness and to identify and address errors and omissions in the datasets.

2.2. Study area

The area of study of this work is the plain of Chania, one of the most intensively cultivated and agriculturally productive areas of Crete, located in the northeastern part of the island. The study area, which occupies about 215 km^2, includes the main parts of the Keritis and Tavronitis basins. These particular catchment areas, are catalytically contributing to the water potential of the wider area of Chania. The main crops cultivated in the area are olive and citrus trees, the products of which supply a large part of the domestic and international markets. This is an especially important agricultural area, not only for Crete but also at the national level, contributing to the viability of the Greek agricultural economy (Kourgialas et al., 2017).

In the wider study area, the topographic relief (Fig. 2A) varies significantly, with the maximum altitude reaching 798 m in the south and the minimum in the northern part (coastline), where the rivers Keritis and Tavronitis discharge to the sea. The southern part of the study area is semi-mountainous and hilly with a relatively dense hydrographic network. The northern part is flat with rich vegetation and water availability. The study area includes approximately 22 km^2 of cultivated citrus groves mostly located in the lowlands (0–200 m) and 119 km^2 of arable land where olive trees are cultivated, located both in the lowlands (0–200 m) and the semi-mountainous areas (200–800 m). The land use map of the study area was digitized in a GIS environment, based on satellite images of geoinformation services of the Ministry of Agriculture of Greece as well as CORINE Land Cover 2006 databases.

2.3. Data collection and analysis

2.3.1. Meteorological data

Precipitation data were collected from the following institutions: a) H.A.O.-DEMETER (Institute of Olive Tree, Subtropical Crops and Viticulture-Chania), b) Technical University of Crete -School of Environmental Engineering and c) Prefectural Administration of Chania. Seven meteorological stations were selected located either within or adjacent to the study area, so that their spatial distribution fully covers the spatial variation of rainfall in the area (Fig. 2A). The meteorological data cover a period of 55 years (1960–2015) at daily time step. Based on the station elevations, three out of the seven are distributed in the semi-mountainous areas (Prasses at 520 m a.s.l., Palia Roumata at 316 m a.s.l., and Zimvragou at 235 m a.s.l.) and four are distributed in the lowlands (Alikianos at 66 m a.s.l., Drapania at 22 m a.s.l., Agrokipio at 8 m a.s.l., and Tavronitis at 16 m a.s.l.). The largest annual rainfall is observed at

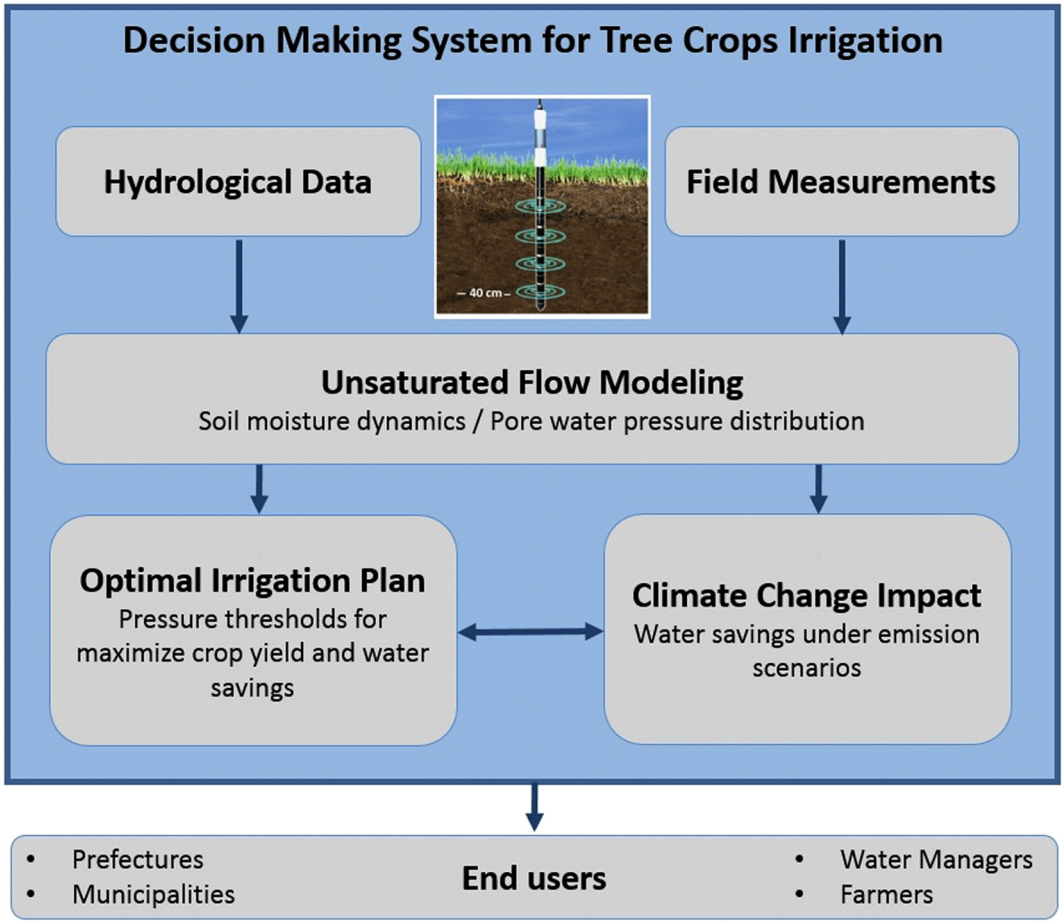

Fig. 1. Flow chart of the proposed methodology.

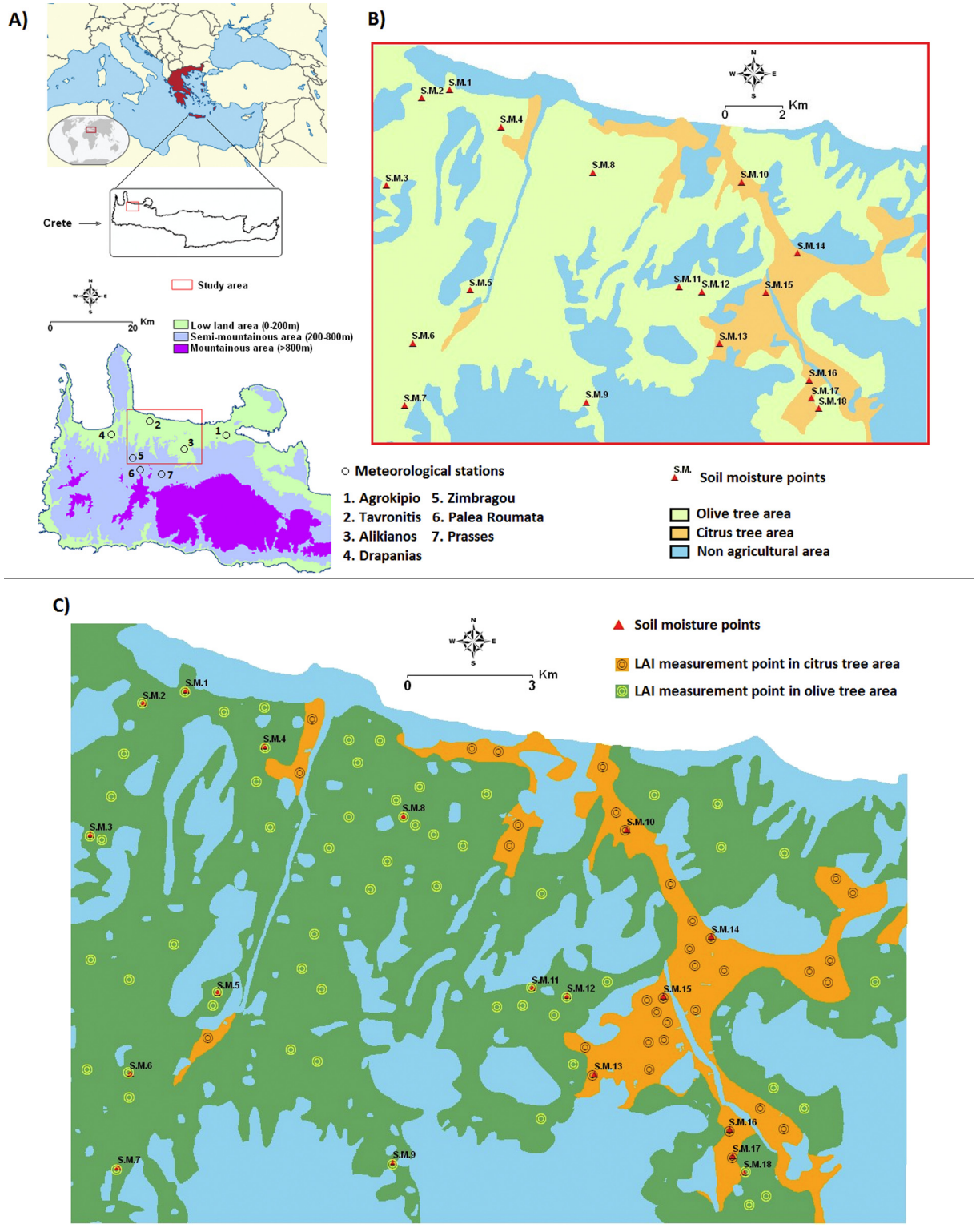

Fig. 2. A) Study area and meteorological stations, B) soil moisture measurement points and land uses, C) LAI measurements points.

the Prasse meteorological station (1860 mm) while the lowest at Tavronitis station (670 mm).

The total precipitation in the study area, based on the above data, takes place between October and March, with the rainiest months being January and February. On the contrary, July and August are dry months across the lowlands. The average number of rainy days is estimated at approximately 90 days. In the semi-mountainous part of the study area, significant rainfall as well as snowfall is observed. With regard to temperatures, the area generally has relatively high temperatures in the summer and temperature fluctuations in the winter are smooth. In the lowlands of the basin, the average minimum temperature, observed in the months of January–February, is about 9.2 °C, while the average peak occurs in July and reaches 30.3 °C (Kourgialas et al., 2016). The precipitation, temperature and reference evapotranspiration data used in the proposed modeling approach were obtained from the seven meteorological stations in the study area. The model

requires actual crop evapotranspiration as input. Using the reference evapotranspiration (ET_o) data, the actual crop evapotranspiration (ET) for citrus and olive crops was estimated, using the following equation (DHI, 2011):

$$ET = k_c ET_0$$

The plant coefficient (k_c) in the above equation depends on time and the type of crop. This factor changes during the germination period. In our case, considering that in the simulation area the dominant crops are those citrus and olive trees ꞇhe plant coefficient ranged, during May to September, from 0.6 to 0.7 for citrus and from 0.4 to 0.45 for olive trees. These accurate time variation values of kc were obtained by experimental works that took place for the specific crops in the Prefecture of Chania by H.A.O.-DEMETER (Institute of Olive Tree, Subtropical Crops and Viticulture-Chania) (Chartzoulakis et al., 1999, 2001). These values are also in agreement with the corresponding general values of FAO 2000 and 2011.

2.3.2. Soil moisture data

A monitoring network for measuring the soil moisture profile with depth was installed at 18 locations within the study area (Fig. 2B). The installation was carried out in both citrus (6 locations) and olive grove fields (12 locations). More specifically, in an area of approximately 215 km^2 (study area), a total of 18 access tubes (T-Devices PR2), each 50 cm long, were installed. With the help of special drills, a hole of 2.5 cm in diameter was created in the soil profile up to a depth of 50 cm in order to place the access tubes. The tubes were sealed externally with a plastic cap, which was only opened when measuring soil moisture with the Profile Probe (Delta T-Devices PR2 - HH2). This device features 4 sensors measuring soil moisture at 4 different soil depths (10, 20, 30 and 40 cm). The advantage of the particular soil moisture sensor is that it simultaneously provides soil moisture measurements at various depths with high accuracy and with minimum disturbance of the soil substrate. Soil moisture measurements were taken at intervals of 1 to 10 days to account for the variability of soil moisture content based on various meteorological conditions. Fig. 2C shows the spatial distribution of the soil moisture measurement locations (S.M.1–18) with respect to the land use coverage.

The criteria for determining the installation locations of the soil moisture recording system were the following: a) adequate spatial coverage of the olive and citrus tree crops within the study area, b) establishment of a soil moisture measurement network in both the lowland and the semi-mountainous zone and c) ability to record measurements at different soil types found within the study area.

2.3.3. Leaf area index (LAI) data

Leaf area index (LAI) measurements were collected on a total of 35 citrus trees and 60 olive trees within the study area. The selection of these trees was made so that their spatial distribution covered the studied area as well as the 18 soil moisture measurement points S.M. (1–18). Also the aim was to record the foliage index in trees of both the lowland and the semi-mountainous zones, covering, as much as possible, the variation of the leaf surface on the different trees (olives - citrus) in relation to their age and the particular topographical and climatic conditions of the various sub-parcels of the study area. The spatial distribution of the measurement points for LAI is illustrated in Fig. 2C. The same figure shows the spatial distribution of the different crops (olives - citrus trees) as well as the soil moisture locations. Based on the Leaf area index (LAI) measurements, in the case of citrus fruits, the average LAI was 3.2 and for olive groves 2.9. These values of LAI were used as input in the modeling simulation.

2.3.4. Laboratory analysis of soil samples

In order to determine the mechanical composition and hydraulic characteristics of the soils within the study area, composite soil samples were taken at 18 locations, coinciding with the soil moisture measurement locations. More specifically, four soil samples were collected at 0–30 cm depths at each of the soil moisture locations (S.M.1–18), which were then placed in a sampling bag to produce a composite sample for each location. The samples were analyzed to determine the a) mechanical composition, b) soil organic matter content, c) pH and d) electrical conductivity.

The determination of the granulometric composition of the soils was carried out using the Bouyoucos method (Bouyoucos, 1962). The Walkley-Black method (1934) was used to determine the soil organic matter content. The pH determination was performed using a pH meter and the electrical conductivity was determined using a conductivity meter. The soil type classification of soil samples was based on the percentage of sand, clay and silt particles expressed in percentages. Based on the U.S. soil classification system of the Department of Agriculture and the mechanical analysis described above, the soil type for each of the 18 soil samples was determined. A summary of the results of mechanical analysis, organic matter, pH, and electrical conductivity (EC) of the studied soil samples are described in Table 1.

According to River Basin Management Plans GR13 (2015) the olive and citrus crops, in the study area, are located in 4 different soil types (loam, sandy loam, loamy sand, sandy clay loam). The mechanical composition of the 18 soil sample described above, verifies the spatial distribution of the four main soil types in the study area. Twarakavi et al., 2010, used a methodology to determine an average value and a corresponding standard deviation of the hydraulic parameters for 12

Table 1
Mechanical analysis results for the 18 soil samples.

Measurement point	Soil type	Sand (%)	Clay (%)	Silt (%)	pH	EC (μS/cm)	Organic matter (%)
S.M.1	Loam	39.20	21.52	39.28	7.18	175.30	2.88
S.M.2	Loam	38.48	19.52	42.00	8.12	325.00	2.88
S.M.3	Loam	38.48	16.52	45.00	8.32	249.00	5.09
S.M.4	Loam	37.90	19.20	42.90	7.90	312.00	2.95
S.M.5	Sandy loam	39.40	16.04	55.44	8.16	250.00	5.07
S.M.6	Sandy loam	34.80	15.40	50.20	8.22	226.00	4.98
S.M.7	Loamy sand	79.20	5.90	14.90	7.50	211.00	3.25
S.M.8	Loam	39.10	17.60	43.30	7.82	286.30	2.35
S.M.9	Loamy sand	78.80	7.02	14.18	7.42	252.00	3.14
S.M.10	Loam	48.50	16.80	34.70	7.09	197.00	3.95
S.M.11	Loamy sand	77.20	6.52	16.28	7.69	236.00	3.22
S.M.12	Sandy loam	74.20	10.16	15.64	7.11	349.00	2.75
S.M.13	Sandy clay loam	49.80	33.10	17.10	7.25	180.30	3.02
S.M.14	Sandy clay loam	51.50	33.90	14.60	7.37	181.00	1.88
S.M.15	Loam	51.20	11.52	37.28	7.20	179.40	4.42
S.M.16	Sandy loam	65.20	13.16	21.64	6.62	185.90	5.09
S.M.17	Sandy loam	68.48	9.52	22.00	6.39	382.00	4.15
S.M.18	Loam	37.48	21.52	41.00	7.11	194.30	4.42

different soil types, including the ones found in the study area. Using their estimates and considering the results of the mechanical composition of the soil samples collected from the area of interest, the hydraulic characteristics of the soil samples were estimated. Based on Table 1 and the results of Twarakavi et al., 2010, the hydraulic classes of the studied soil samples belong to categories A1, A3, A4 and B2.

2.4. Model development

For the simulation of flow in the unsaturated zone, the model MIKE SHE was used, which is a finite difference model that allows the simulation of all the processes of the hydrological cycle with the use of various modules. In the present study, in order to simulate the flow in the unsaturated zone, we utilized the following modules: a) Flow in the unsaturated zone (UZ) and b) Evapotranspiration (ET). The simulation period was set from 1/9/2014 to 31/5/2015. The model area (study area) was divided into a number of computational cells of size 20 × 20 m.

In this study, in order to accurately simulate the flow in the unsaturated zone, Richards's equation was used. However, to solve Richards's equation, two important relationships need to be defined: the soil-water characteristic curve and the permeability-saturation curve. Unsaturated hydraulic conductivity is one of the most important properties that govern flow in the unsaturated zone; however, it is very difficult to measure experimentally. Knowledge of the highly nonlinear relationship between unsaturated hydraulic conductivity and volumetric water content is required. In this work, the empirical equations of Van Genuchten were used to define the above relationships. For more information on the mathematical equations used by the model the interested reader is referred to the model manual (DHI, 2011).

The Van Genuchten parameters were estimated based on the specific hydraulic classes (A1, A3, A4 and B2) encountered in the area, as define above. Specifically, the following parameters were determined: volumetric water content (θ), residual water content (θr), saturated hydraulic conductivity (K), m = parameter estimated from the soil-water curve, n = adjustment parameter, n = 1 / (1 − m) and a = customization parameter and are presented in Table 2.

The vertical discretization of the unsaturated zone was based on historical data from drilling wells in the wider area of the simulation. Using the Disjunctive kriging method in a GIS environment, a map of the depth of the unsaturated zone for every point of the study area was created. According to this, in the simulation area the average depth of the unsaturated zone is about 10 m below the ground surface. According to the above, the unsaturated zone was divided into 3 soil profiles from 0 to 0.2 m, 0.2–1 m, and > 1 m with a vertical discretization of 0.1 m, 0.2 m and 0.5 m within each of the soil profiles. The selection criteria for this discretization were based on:

a) Higher vertical discretization of the soil depth in the upper layers is needed to capture the zone where the most significant changes in flow occur.

b) The root zone system of both citrus and olive trees is concentrated in the upper soil layers (10–40 cm) (Besharat et al., 2010).

2.5. Climate change scenarios

The impact of climate change was also assessed as part of the decision making system. According to the analysis of meteorological data by Tsanis et al. (2011) for the island of Crete, three different global climatic models GCMs (ECHAM5, IPSL, and CNRM) and two emission scenarios (the highest RCP 8.5 emission and the lowest RCP 4.5 emission) were used in this study. The results of the average monthly rainfall and temperature from the ECHAM5, IPSL, and CNRM climatic models for the time period (2019–2030) were used. This relatively short forecast was chosen to reduce the uncertainty of the results to some extent. According to the results of the aforementioned analysis, for the RCP 4.5 emission scenario, average annual rainfall is expected to increase by 1%, while the average annual temperature is expected to increase by an average of 1.5 °C. In addition, for the RCP 8.5 emission scenario, the average annual rainfall is expected to decrease by 2%, while the average annual temperature is expected to increase by an average of 1.4 °C (Koutroulis et al., 2013).

These forecasts were then incorporated into the stochastic weather generator LARS-WG model (Semenov and Barrow, 1997, 2002) to generate daily future time series data for the 7 meteorological stations in the area of interest (Fig. 2A). These meteorological time series were used as input data in the calibrated and validated hydrological model MIKE SHE to predict water availability and soil moisture dynamics in the studied agricultural areas for the period between 2019 and 2030. The derived temperature time series was converted into daily reference evaporation (ET_o) time series based on empirical equations (Blaney-Criddle equation). For the solar radiation parameter, there are no predictions for the RCP 8.5 and RCP 4.5 emission scenarios, so the statistical analysis of the available solar sunshine time series was performed to generate the trend and then used in all scenarios (RCP 8.5 and RCP 4.5).

3. Results and discussion

3.1. Model calibration and validation

The model was calibrated for the period from September 1st, 2014 to January 31st, 2015, using soil moisture measurements collected at fifteen different times, at eighteen locations in the study area (SM1–18) and at four different depths (10, 20, 30 and 40 cm). During model calibration no irrigation is applied in the study area, since plant watering needs are covered by rainfall. The calibration parameters were the following: Van Genuchten parameters (θs, θr, a, n, Ks), bulk density and initial soil moisture. The calibration process was performed using the AUTOCAL analysis tool, an optimization tool that performs automatic calibration in the MIKE SHE environment.

The validation of the model was performed for the period from February 1st, 2015 to May 31st 2015, for the same eighteen locations in the study area (SM1–18) and for the same four depths with data collected at 14 different times.

Both the calibration and validation of the model were performed during the rainy season in order to capture the variability of soil

Table 2
Mean and standard deviation (in parentheses) of soil hydraulic parameters for different soil hydraulic classes estimated from the Schaap et al. (2001) and Twarakavi et al. (2010) database.

Soil sampling points	Soil hydraulic class	θ_r	θ_s	$\log_{10}(a)$ in $\log_{10}(cm^{-1})$	$\log_{10}(n)$	$\log_{10}(K_s)$ in $\log_{10}(cm/day)$
S.M.7, S.M.9, S.M.11, S.M.12	A2	0.053 (0.002)	0.386 (0.007)	−1.474 (0.076)	0.276 (0.055)	2.093 (0.696)
S.M.1, SM.2, S.M.4, S.M.8, S.M.10, S.M.15- S.M.18	A3	0.051 (0.002)	0.382 (0.01)	−1.54 (0.176)	0.171 (0.015)	1.641 (0.659)
S.M.13, S.M.14	A4	0.055 (0.003)	0.387 (0.009)	−1.672 (0.183)	0.14 (0.019)	1.242 (0.764)
S.M.3, S.M.5, S.M.6	B2	0.053 (0.003)	0.425 (0.03)	−2.278 (0.124)	0.206 (0.024)	1.714 (0.594)

Table 3
Calibration parameters of the modeling simulation.

Soil types	Parameter					
	θr (−)	θs (−)	a (1/cm)	n (−)	Ks (m/s)	ρ (g/lit)
Sandy clay loam (I)	0.055	0.387	0.021	1.38	2e-006	1350
Sandy clay loam (II)	0.055	0.387	0.021	1.38	2e-006	1350
Sandy clay loam (III)	0.055	0.387	0.021	1.38	2e-005	1800
Sandy loam (I)	0.053	0.428	0.0052	1.6	5.991e-006	1350
Sandy loam (II)	0.053	0.428	0.0052	1.6	5.991e-006	1350
Sandy loam (III)	0.053	0.428	0.0052	1.6	5.991e-006	1800
Loam (I)	0.051	0.382	0.028	1.48	5e-006	1350
Loam (II)	0.051	0.382	0.028	1.48	5e-006	1350
Loam (III)	0.051	0.382	0.028	1.48	5e-006	1800
Loamy sand (I)	0.053	0.386	0.033	1.88	1.433e-005	1350
Loamy sand (II)	0.053	0.386	0.033	1.88	1.433e-005	1350
Loamy sand (III)	0.055	0.387	0.021	1.38	1e-025	3800

moisture content as a response to varying meteorological conditions. This was also preferred due to the difficulties in monitoring the time and space variability of applied irrigation in each plot of the study area, which depends on the specific farmer's irrigation practices during the dry season.

For demonstration purposes, the calibration results are shown for two locations, SM8 (Olive trees) and SM13 (Citrus trees). The results of the automatic calibration are shown in Table 3. In this table the soil profiles of 0–0.2 m, 0.2–1 m, and > 1 m are denoted by the symbols (I), (II), (III), respectively. With regard to the initial soil moisture conditions, taking into account the date of initial simulation (1/9/2014) we considered uniform initial soil moisture conditions throughout the study area, determined during the calibration process (0.15 cm^3/cm^3).

During the calibration process the good agreement between the field measurements and the simulation results was demonstrated on the basis of various statistical indicators, indicating a successful calibration process. The metrics considered were the following: Mean error (ME), mean absolute error (MAE), root mean square error (RMSE), standard deviation of the residuals (STDres), and correlation coefficient (R) (Table 4). In all cases (18 measurement points), the values of the correlation coefficient (R) ranged from 0.86 to 0.98. Figs. 3 and 4 illustrate the simulation results (for both calibration and validation) at SM8 (olive tree grove) and SM13 (citrus grove) measurement points with respect to field measurements at soil depths of 10 cm, 20 cm, 30 cm, and 40 cm.

Figs. 5A and B illustrate the soil moisture dynamics in the unsaturated zone at specific locations (SM8 and SM13) for the entire simulation time up to 1.5 m depth. This depth is chosen for illustration purposes and given that the maximum root depth for olive and citrus trees is up to 1.5 m. In October and November, when rainfall has a lower frequency than in the winter, soil moisture is low in the upper layers of the unsaturated zone. However, during December–April, there is a significant increase in soil moisture as a result of increased rainfall. After mid-May there is a gradual decrease in soil moisture in both the upper and lower layers of the unsaturated zone. It was observed that at location SM8 (olive) the soil moisture front moves slower to the deeper layers than the corresponding SM13 (citrus) measurement point. This is mainly attributed to the soil type in these locations, with SM8 located at loam while SM13 at sandy clay loam, which enables faster flow of water through the unsaturated zone.

3.2. Optimal irrigation scenarios

For designing the optimal irrigation plan the following information is critical: (a) the variation in soil moisture at any point in the study area, which in turn can be translated into pore water pressure in the unsaturated zone relative to the soil depth, and (b) the threshold within which the optimal irrigation time, frequency and application rate can be determined for obtaining satisfactory yields of olive and citrus trees (Blaney and Criddle, 1962).

Based on the results of the modeling and in particular the variation of pressure with depth, the correct time for applying irrigation can be determined, with a view of saving water resources and optimizing the yield of the respective crops. According to the literature, for optimum plant growth and yield, the pressure for citrus trees must be maintained throughout the year over −5 m, at the soil depth of 30 cm. Respectively for olives, the pressure in relation to the soil depth should be kept above −100 m, while in the period April–May (blossoming stage) and September–October (fruit ripening - oil accumulation stage) it should be kept above −30 m at the soil depth of 30 cm. It should be noted here that the olive trees are particularly sensitive to the lack of water during blossoming, which may cause flowering and production decline (Michelakis et al., 1996; Shirgure, 2013; Kourgialas and Karatzas, 2015; Koubouris et al., 2015).

The critical pore water pressure values for both citrus and olives at the soil depth of 30 cm are presented in Figs. 6A (SM8) and 6B (SM13) by a red line. Based on the pressure thresholds for optimum

Table 4
Statistical comparison between soil moisture measurements at locations SM8 (olive trees) and SM13 (citrus trees).

Location	Number of field measurements taken in time	ME	MAE	RMSE	STDres	R
Calibration						
SM8 (10 cm)	15	0.004	0.010	0.014	0.013	0.988
SM8 (20 cm)	15	0.001	0.007	0.011	0.011	0.991
SM8 (30 cm)	15	0.002	0.005	0.008	0.008	0.995
SM8 (40 cm)	15	0.002	0.004	0.008	0.007	0.996
Validation						
SM8 (10 cm)	14	0.009	0.010	0.013	0.008	0.978
SM8 (20 cm)	14	0.006	0.013	0.012	0.007	0.981
SM8 (30 cm)	14	0.003	0.005	0.010	0.011	0.987
SM8 (40 cm)	14	−0.001	0.005	0.009	0.006	0.990
Calibration						
SM13 (10 cm)	15	−0.008	0.012	0.018	0.016	0.984
SM13 (20 cm)	15	−0.001	0.006	0.007	0.007	0.997
SM13 (30 cm)	15	0.000	0.007	0.008	0.008	0.995
SM13 (40 cm)	15	0.000	0.005	0.009	0.009	0.996
Validation						
SM13 (10 cm)	14	0.010	0.010	0.013	0.008	0.977
SM13 (20 cm)	14	0.009	0.010	0.011	0.006	0.988
SM13 (30 cm)	14	−0.001	0.004	0.008	0.006	0.990
SM13 (40 cm)	14	−0.009	0.006	0.009	0.008	0.989

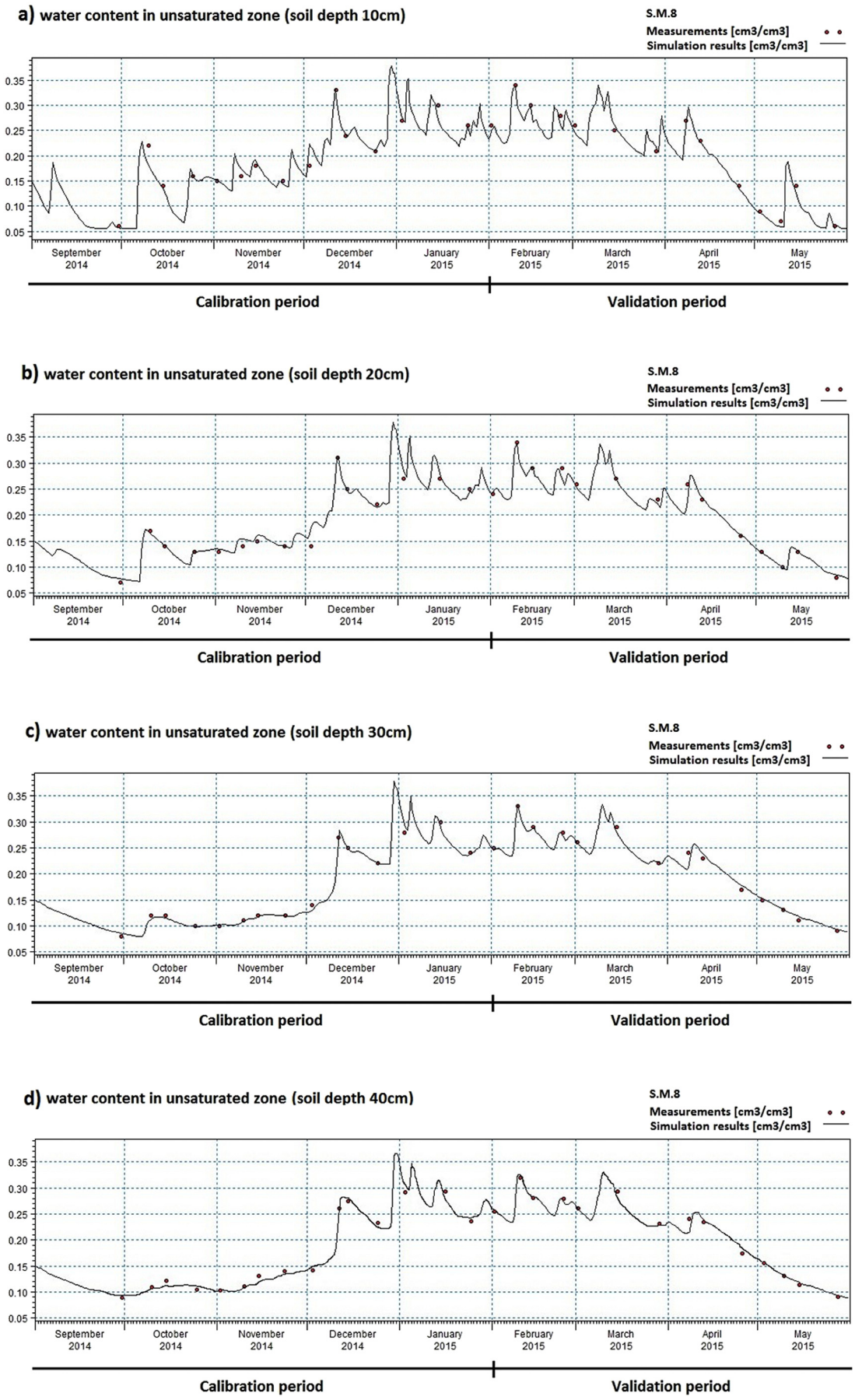

Fig. 3. Soil water content - calibration and validation results at location SM8.

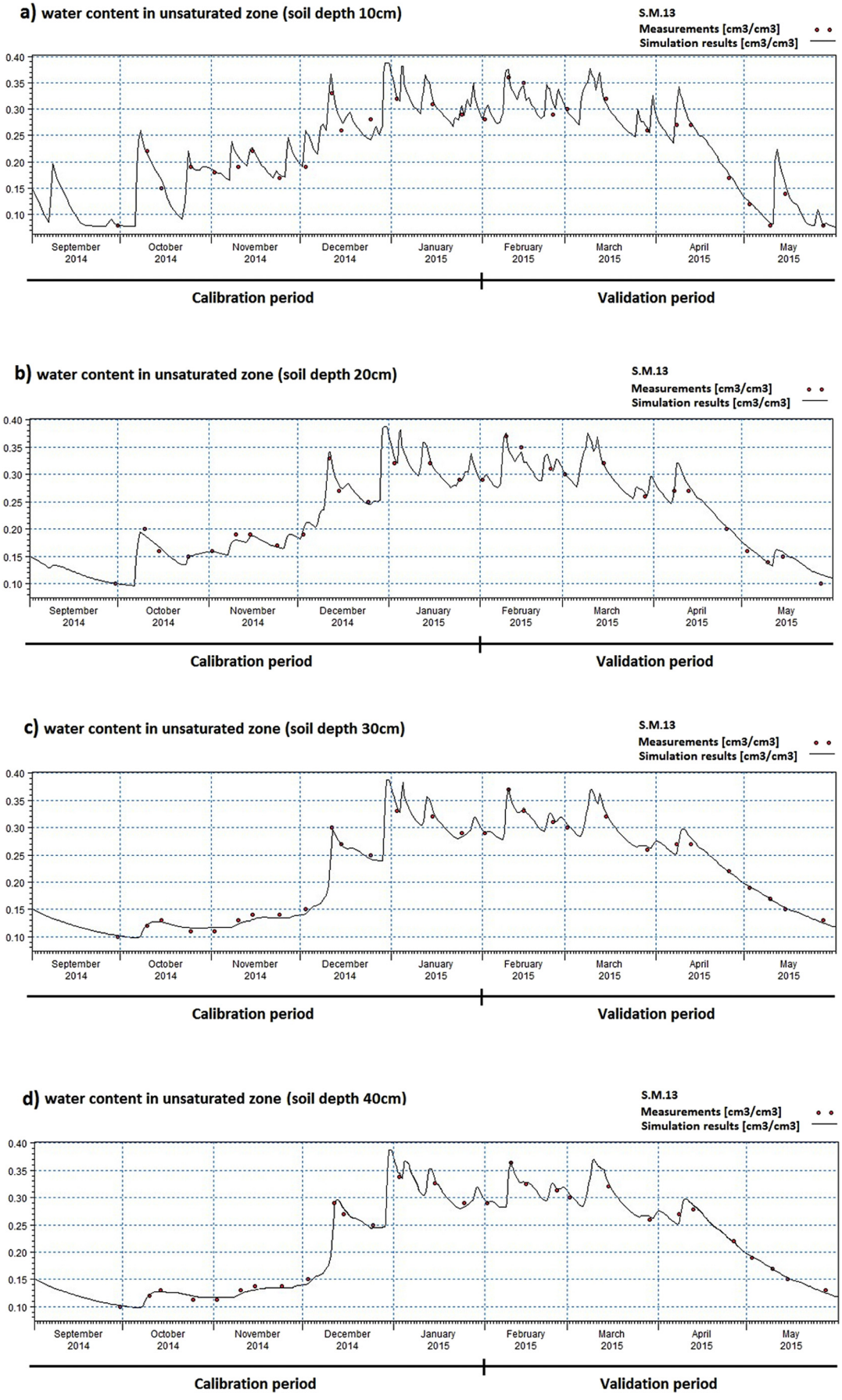

Fig. 4. Soil water content - calibration and validation results at location SM13.

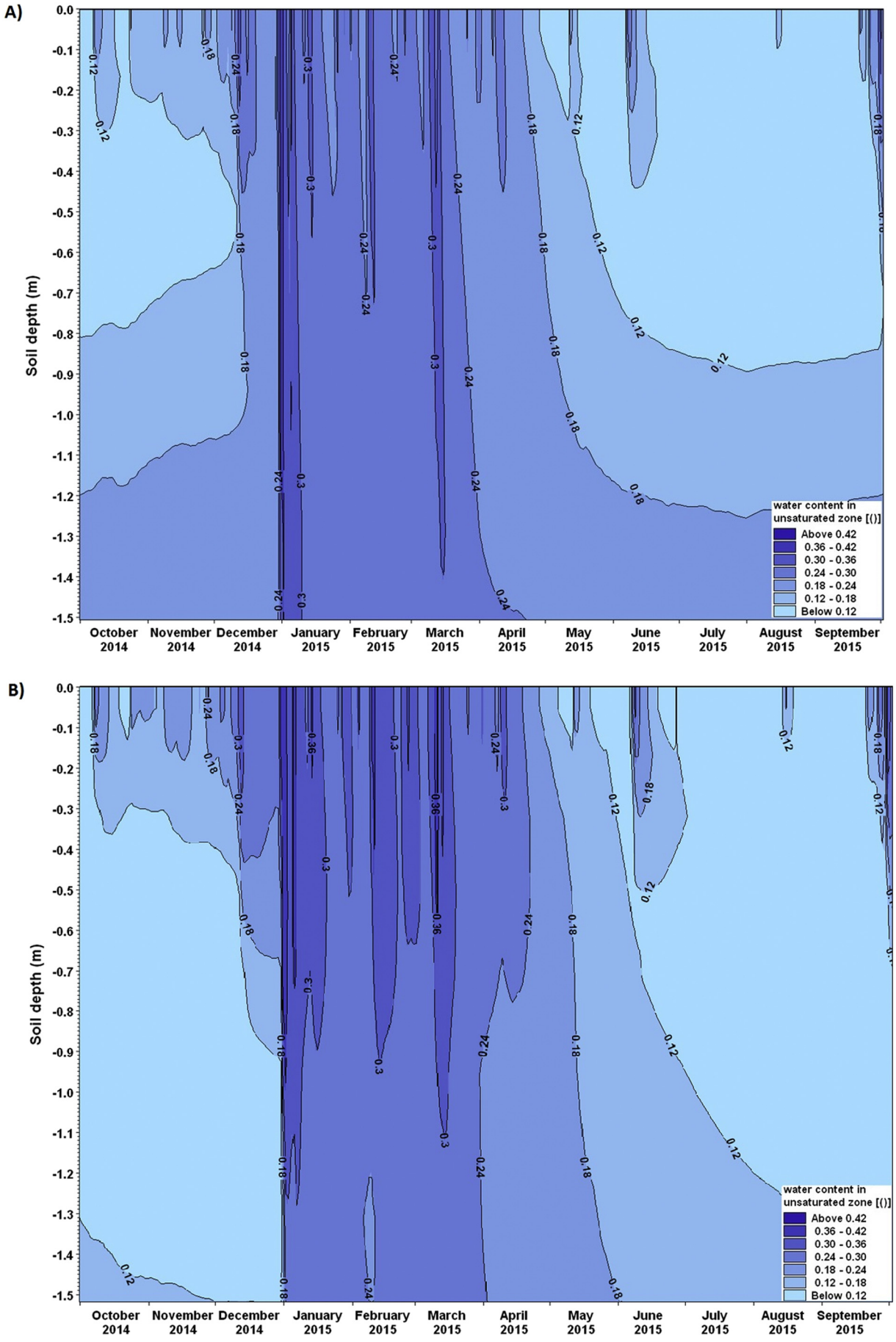

Fig. 5. Soil moisture dynamics with depth, A) SM 8 (olive tree area) and B) SM13 (citrus tree area) locations.

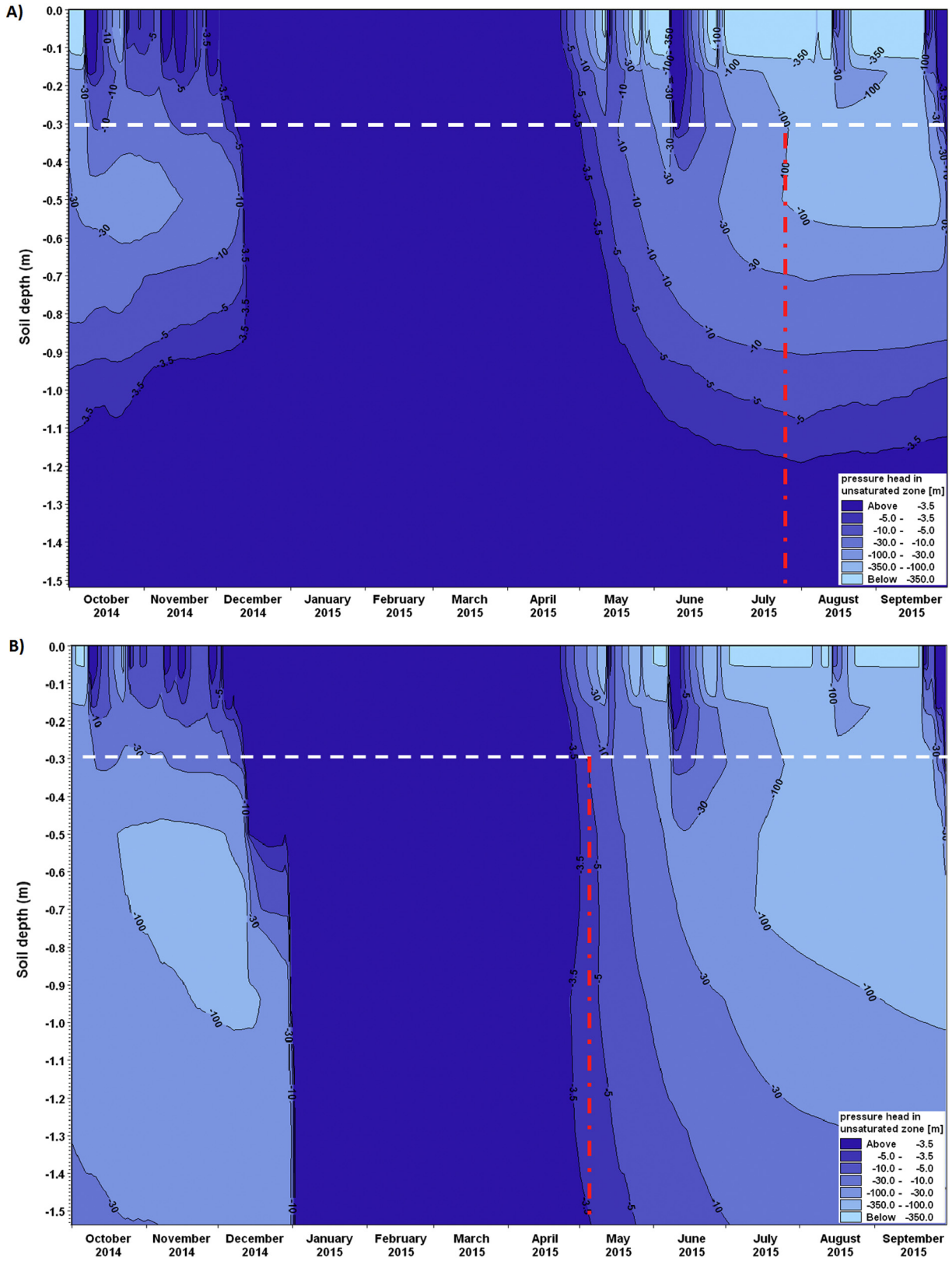

Fig. 6. Pressure head dynamics with respect to soil depth and onset of irrigation based on pressure head at soil depth of 0.3 m for A) SM 8 and B) SM13 locations. Based on thresholds, the proposed start of irrigation is Mid July for SM 8 (olive trees) and late April for SM13 (citrus trees).

yield of the studied crops, we have implemented different irrigation scenarios to achieve the lowest water application while maintaining the pressure within the required limits for each crop. The optimal irrigation scenario was found through trial and error. Figs. 7A and B show the optimum irrigation water application scenarios for SM8 (olive trees) and SM13 (citrus), respectively. For the study area SM8 (olive trees) and for the simulated meteorological conditions, the optimal irrigation scenario was to apply irrigation water starting in July 20th, at a rate of

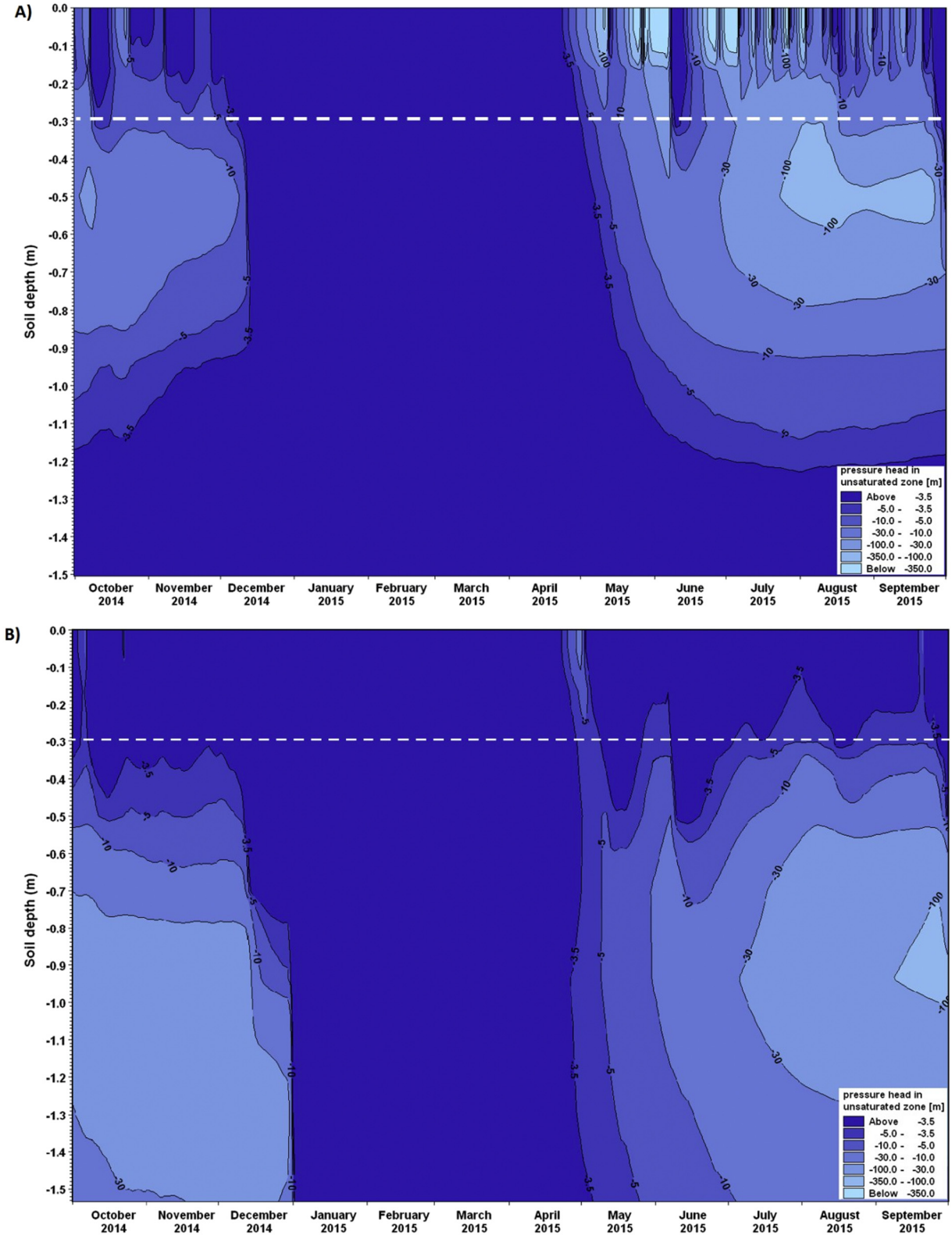

Fig. 7. Results when applying the optimal irrigation plan determined above at A) SM 8 and B) SM 13 locations. Pressure head is kept above the thresholds.

80 m^3 Ha^{-1}per week until the end of August, and then until mid-September the rate is 70 m^3 Ha^{-1}, per week. No further irrigation was required after September, 15th.

For SM13 and for the simulated meteorological conditions, the optimal irrigation scenario was to apply irrigation water starting in May 9th, at a rate of 10 m^3 Ha^{-1} on a daily basis until the end of the May, and from June 1st to mid-September the optimal rate is 20 m^3 Ha^{-1} on a daily basis. No further irrigation was required after the 15th of September. Based on the typical irrigation practices for the May–September 2015 period for both olive trees (3000 m^3 Ha^{-1}) and citrus trees

(4500 m^3 Ha^{-1}), the irrigation water savings that can be achieved by applying the proposed methodology are 41% and 36%, for SM8 (olive trees) and SM13 (citrus), respectively.

Taking into consideration that in the study area the water price per m^3 is equal to 0.17 euro, the total water consumption cost based on typical irrigation practices (both for citrus and olive trees) is equal to 7,752,000 euro, while for the proposed optimal irrigation scenario in the study area (both for citrus and olive trees) it is equal to 3,094,170 euro. Thus, the proposed methodology is also preferable in terms of cost, saving about 40% of the typical water consumption cost for irrigation in the study area.

The results with regard to optimal irrigation scenarios also indicated that in the case of olive groves, the amount of irrigation water applied on a weekly basis can maintain the pore water pressure in the unsaturated zone within the acceptable limits, in contrast to citrus trees, where irrigation applied more frequently is preferable.

3.3. Water management of olive and citrus crops under climate change scenarios

Based on the simulation results of the MIKE SHE model, maps (for each computational cell, Y direction corresponds to soil depth and X

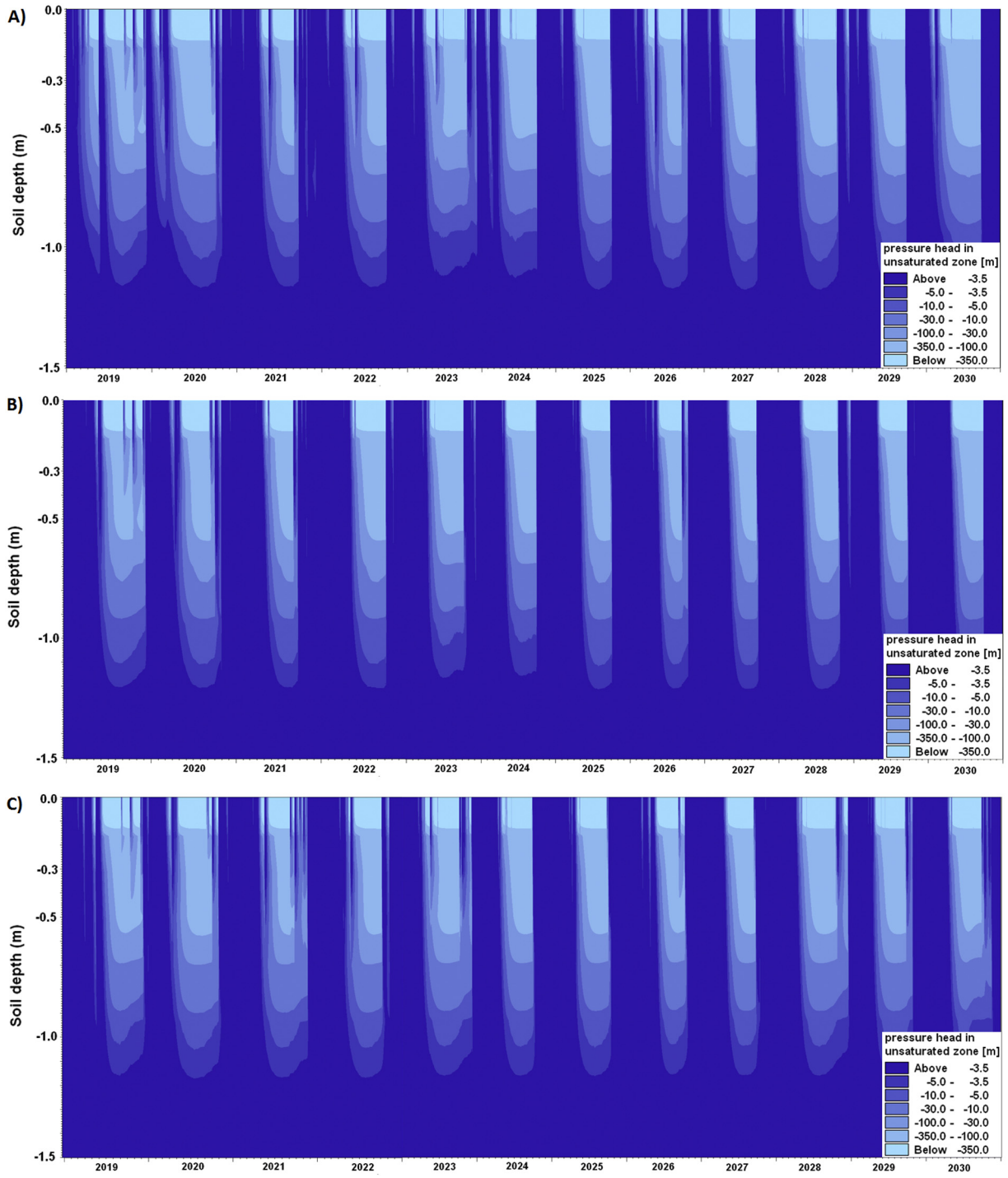

Fig. 8. Pressure head dynamic with soil depth at SM 8 location based on: A) RCP 8.5 climate change scenario, B) RCP 4.5 climate change scenario, and C) Baseline climate scenario, (period 2019–2030).

direction corresponds to time) of the pore water pressure distribution in the unsaturated zone with respect to the soil depth, at each point of the study area, for the period (2019–2030) and for the climatic scenarios Baseline, RCP 8.5 and RCP 4.5 (Figs. 8 and 9) were produced. This allows to optimize the planning of irrigation needs for the next 11 years, for any part of the study area (olive and citrus crops).

Table 5 presents the maximum percentage of irrigation water savings (compared to the usual irrigation practices) at SM8 (olive trees) and SM13 (citrus) locations for the period 2019–2030. The results show that when the summer period is relatively mild or wet the water saving rates are high compared to the case of severe dry conditions, as was expected. Indicatively, according to the forecasting scenarios, for the wet years 2027 and 2029 significant irrigation water savings (in relation to normal irrigation practices) are observed both at SM8 (olive trees) and SM13 (citrus). In contrast, according to forecasting scenarios, in dry years such as 2019 and 2020, irrigation water savings rates are much smaller. Considering the possibility of saving irrigation water for the time period (2019–2030), on average the lowest savings rates were observed for the emission scenario (RCP 8.5) with rates of 29.2% and 25.2% for SM8 (olive trees) and SM13 (citrus), respectively. The Baseline scenario follows with 34.8% and 30.6% for SM8 (olive trees) and SM13 (citrus), respectively. While for the lower

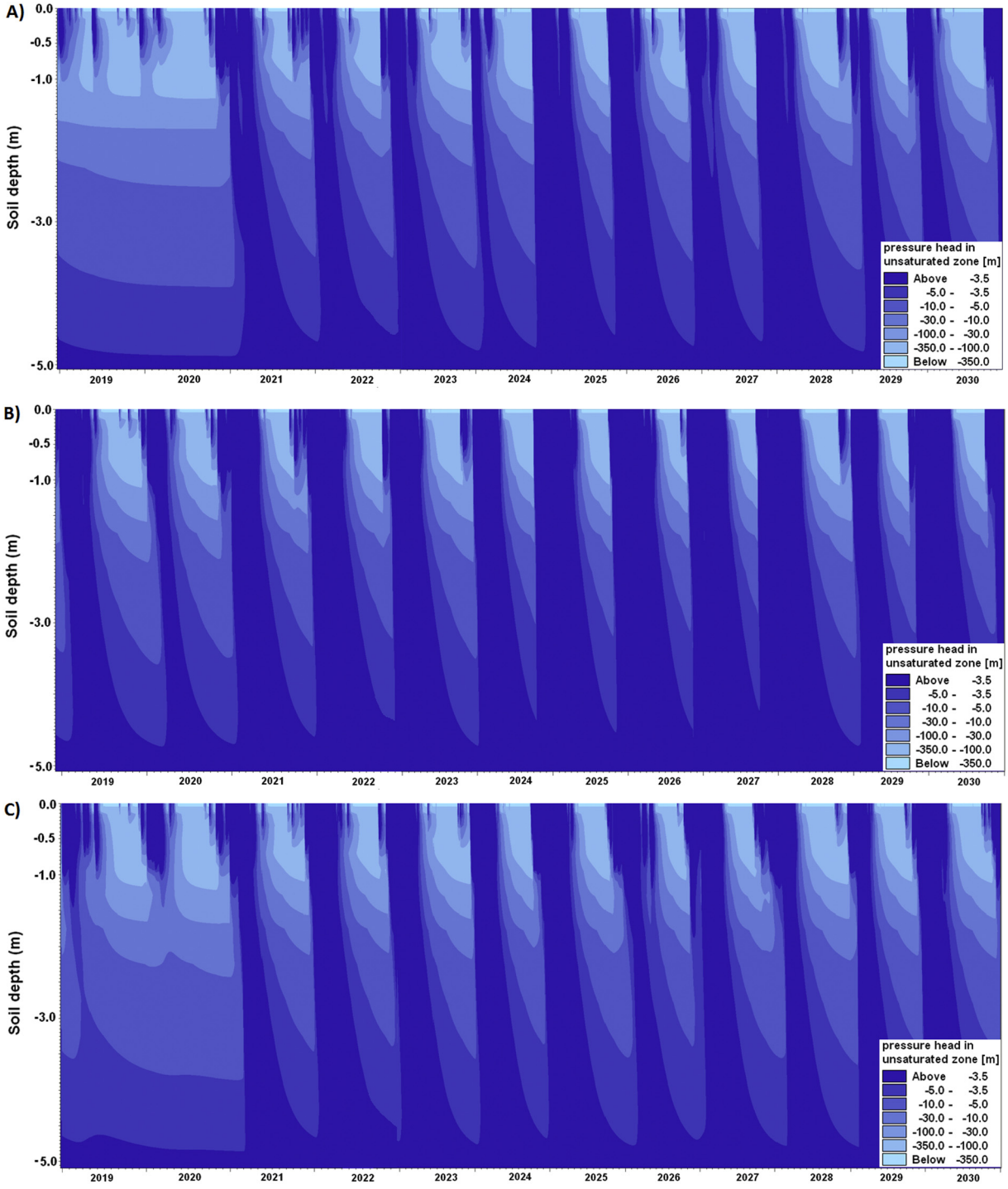

Fig. 9. Pressure head dynamic with soil depth at SM 13 location based on: A) RCP 8.5 climate change scenario, B) RCP 4.5 climate change scenario, and C) Baseline climate scenario, (period 2019–2030).

emission scenario (RCP 4.5) the percentages reached 53.3% and 46.7% at SM8 (olive trees) and SM13 (citrus), respectively. As observed in Table 5, in general, the largest water savings can be achieved for olive tree crops under all three climatic scenarios. This is due to the fact that olive trees require less irrigation water compared to citrus trees.

In line with the above, in the case of the low emission scenario (RCP 4.5), and in particular for the years 2024, 2027 and 2029, where the respective rainfall (1537, 1721 and 2164 mm) amount and intensity are high, the irrigation water saving rates are expected to increase in the following order of years: 2024, 2027 and 2029. The above is indeed observed at the site SM8 (olive trees) with high irrigation water saving rates for the years 2024, 2027 and 2029 reaching 67%, 70% and 71%, respectively. However, in the case of citrus trees (SM13) for the years 2024, 2027 and 2029, saving rates are similar reaching 61%, 60% and 59%, respectively.

This differentiation in the case of citrus trees is due to the fact that their optimum growth is ensured if the soil moisture pressure is maintained at high levels (−5 m at the soil depth of 30 cm) throughout the year. In the case of the lower emission scenario (RCP 4.5), which predicts high amounts and intensities of rainfall (especially in the autumn and spring), deep percolation under the root system of the plants is expected. This phenomenon does not contribute to keeping the pressure at levels above −5 m. Thus, for the SM13 site (citrus) while there is plenty of rainfall water in ascending order for the years 2024, 2027 and 2029, the irrigation water savings do not follow the same order, but remain relatively stable.

With regard to the climatic scenario results shown in Figs. 8 and 9, years 2019–2020 are expected to be dry (under all scenarios) with lower pressure values in the unsaturated zone. Particularly, in Fig. 9 (SM13 - citrus) this phenomenon is more prevalent compared to point SM8 (Fig. 8) for the same depth, possibly because SM13 is located in an area where the water table (zero pressure) is low and the unsaturated zone depth is high, while point SM8 is located at an area where the water table is higher (smaller unsaturated depth). In general, the desired pressure thresholds for optimal irrigation are easier to achieve in locations where the water table is high, resulting in larger water savings.

It should be noted that, although results are presented only for locations SM8 and SM13 here, the same conclusions can be drawn for the rest of the area cultivated by olive or citrus trees. Using the proposed decision making system, a comprehensive water management plan for the irrigation needs of the studied agricultural area can be designed for the next decade, contributing to climate adaptation plans adopted by the water managers and other stakeholders in the area.

3.4. Limitations and strengths of the proposed decision making tool

One of the main limitations of using an unsaturated flow model is the uncertainty that arises from model parameterization. In order to address this issue, a sensitivity analysis of the most influential parameters i.e. the Ks Van Genuchten parameter, the bulk density (BD) and the initial soil moisture (ISM) was performed in this study. The above parameters were chosen because they exhibit the most uncertainty among the input data. Specifically, Ks exhibits the highest standard deviation among the other Van Genuchten parameters that were used, while bulk density (BD) and initial soil moisture (ISM) exhibit significant uncertainty due to their spatial variability in the study area. The objective is to study how the uncertainty in these three factors affects the statistical metrics of the model calibration and validation processes. For this propose, reasonable perturbation percentages (±10% and ±20%) were applied to the above calibrated parameter values and the change of the RMSE statistical metric for each studied soil depth and for locations SM8 (olive trees) and SM13 (citrus trees) was computed. Fig. 10 presents the % change of RMSE for each parameter (Ks, BD, ISM). The results show that for the Ks parameter, the applied perturbation percentages have the largest impact on the final results that reaches 7.62% for the calibration period and 10.34% for the validation period. This effect is extenuated with depth, as can be seen in Fig. 10. In the case of the other two parameters, bulk density (BD) and initial soil moisture (ISM), the RMSE changes were relatively small and not >1.3% for all soil depths, time periods (calibration and validation) and locations. Based on the above, in our study it is evident that Ks is the most sensitive parameter, a fact that is consistent with previous studies (Mertens et al., 2005; Seferou et al., 2013). Another source of uncertainty is introduced by the relatively short simulation period for which soil moisture data are available which may affect the reliability of the results. However, the climatic scenarios were based on an extensive meteorological dataset which spans 55 years, thus there is increased confidence on the results associated with the climatic projections.

The pilot study of the decision making system described in this paper uses a catchment scale, high resolution modeling tool to produce results that are relevant at farm scale. This work has the potential to be upscaled to regional scale or transferred to other regions, so that it can be more effectively used for decision making at the Prefecture or national levels. Challenges that may prevent scalability of such modeling schemes are the difficulty of establishing an extensive monitoring network on large scale and long computational times of the unsaturated model. To overcome the first challenge, satellite remote sensing datasets could be used as model forcings of precipitation (eg. IMERG)

Table 5
Estimation of water savings achieved by the optimal irrigation plan (compared to the usual irrigation practices) at locations SM8 (olive trees) and SM13 (citrus) for the period 2019–2030 and under the Baseline, RCP 8.5 and RCP 4.5 scenarios.

Scenarios	Baseline		RCP 8.5		RCP 4.5	
Year	SM8 (olive trees) [%]	SM13 (citrus trees) [%]	SM8 (olive trees) [%]	SM13 (citrus trees) [%]	SM8 (olive trees) [%]	SM13 (citrus trees) [%]
2019	20	18	12	9	21	19
2020	27	24	23	17	36	32
2021	41	36	35	31	58	51
2022	39	34	33	29	53	47
2023	31	28	21	19	44	38
2024	42	37	44	37	67	61
2025	39	34	37	33	66	59
2026	32	28	27	24	51	44
2027	40	35	38	34	70	60
2028	27	24	18	15	47	41
2029	48	42	38	33	71	59
2030	31	27	24	21	56	49
	Average	Average	Average	Average	Average	Average
2019–2030	34.8	30.6	29.2	25.2	53.3	46.7

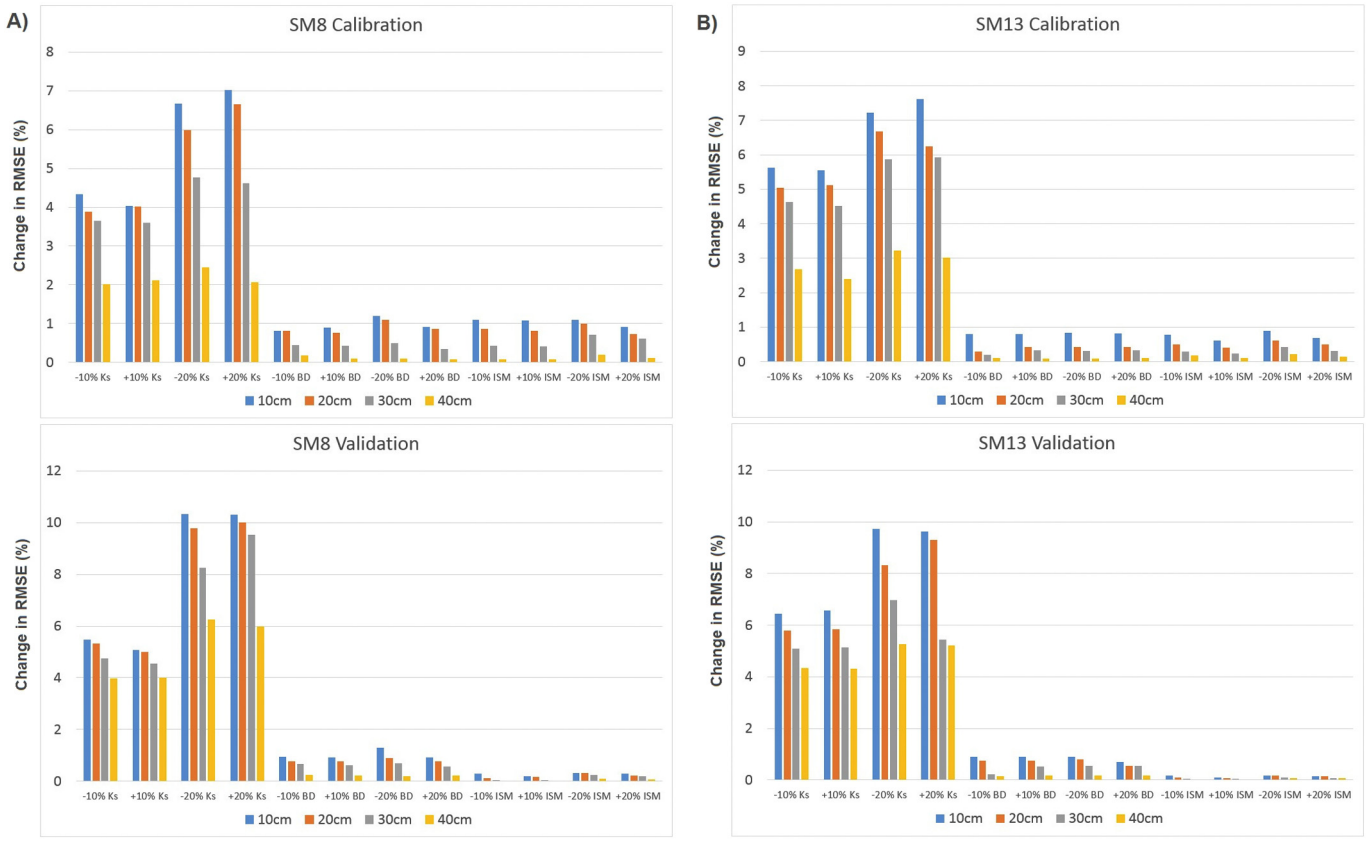

Fig. 10. Sensitivity analysis for A) the calibration period, B) the validation period, for points SM8 (olive trees) and SM13 (citrus trees).

and evapotranspiration (eg. MODIS), after being evaluated locally against ground-based observations. The soil moisture results derived from the unsaturated model could be further validated at a larger scale with satellite soil moisture data (e.g SMAP) in addition to local measurements obtained by a carefully designed soil moisture monitoring network, such as the one described in this work. High temporal resolution information at catchment-scale could also be provided by emerging wireless sensor network technologies [e.g., Cardell-Oliver et al., 2005]. To overcome the second challenge, a high performance computing (HPC) system could be used to run the unsaturated zone model, to reduce simulation times and increase accuracy.

4. Conclusions

The proposed decision-making system allows to continuously monitor soil moisture and pressure in the unsaturated zone at any point in the simulated area and at the same time to develop optimal irrigation plans for olive and citrus crops. In particular, knowing: a) the pressure variation in the unsaturated zone with respect to the soil depth and b) the threshold within which the expected yield for the olive and citrus trees remains appropriate, scenarios of optimal application of irrigation water at any point in the study area can be defined.

Based on the stochastic simulation and predictive meteorological algorithm, the irrigation water management in the context of climate scenarios was also studied. More specifically, through the application of the MIKE SHE calibrated/validated model and based on the RCP 8.5, RCP 4.5 global climatic scenarios and the Baseline scenario, the potential water savings of irrigation water for olive and citrus crops was assessed for the next 11 years (2019–2030).

Based on the results of this work it is shown that when the summer period is relatively mild or wet the irrigation water savings are more significant compared to the case of severe dry conditions, as is expected. Assessing the possibility of saving irrigation water for the time period (2019–2030) and for the Baseline, RCP 8.5 and RCP 4.5 climatic scenarios, it is observed that on average the lowest savings rates are observed in the emission scenario RCP 8.5, followed by the Baseline and the emission scenario RCP 4.5. Also, of interest is that under scenario RCP 4.5, which predicts high rainfall amounts and intensities, more significant deep percolation under the root system of the plants is observed.

The study shows how the design of an optimal irrigation management plan based on state-of-the-art measurement and modeling tools, can effectively contribute towards water saving efforts and potentially address the water scarcity issue in the region, which is becoming pivotal for the viability of agriculture in Crete as also in many other Mediterranean areas. The significant water savings predicted under current and future climatic conditions suggest that the proposed tool would be very beneficial to local stakeholders, if implemented operationally. To this end, it is important to effectively transfer this decision making tool to the relevant stakeholders and water managers and focus on capacity building by providing the appropriate training, in order to ensure the sustainable use of this decision making tool by these and other relevant organizations.

Acknowledgments

This research project is funded under the Action “Research & Technology Development Innovation projects (AgroETAK)”. It is cofounded by the European Social Fund and by National Resources (National Strategic Reference Framework 2007–2013). Coordinated by the Hellenic Agricultural Organization “DEMETER” - Institute of Olive Tree, Subtropical Crops and Viticulture.

References

Bardossy, A., Bogardi, I., Matyasovszky, I., 2005. Fuzzy rule-based downscaling of precipitation. Theor. Appl. Climatol. 82 (1–2), 119–129.

Besharat, S., Nazemi, A.H., Sadraddini, A.A., 2010. Parametric modeling of root length density and root water uptake in unsaturated soil. Turk. J. Agric. For. 34, 439–449.
Blaney, H.F., Criddle, W.D., 1962. Determining consumptive use and irrigation water requirements. USDA Technical Bulletin 1275. US Department of Agriculture, Beltsville.
Bouyoucos, G., 1962. Hydrometer method improved for making particle size analyses of soils. Agron. J. 54, 464–465.
Cardell-Oliver, R., Kranz, M., Smettem, K., Mayer, K., 2005. A reactive soil moisture sensor network: design and field evaluation. Int. J. Distrib. Sens. Netw. 1, 149–162. https://doi.org/10.1080/15501320590966422.
Chartzoulakis, K., Michelakis, N., Stefanoudaki, E., 1999. Water use, growth, yieldand fruit quality of 'bonanza' oranges under different soil water. Adv. Hortic. Sci. 13, 6–11.
Chartzoulakis, K.S., Paranychianakis, N.V., Angelakis, A.N., 2001. Water resources management in the island of Crete, Greece, with emphasis on the agricultural use. Water Policy 3, 193–205.
CORINE, 2016. Land Cover 2006 for Greece. European Environmental Agency.
DHI, 2011. MIKE SHE: an integrated hydrological modelling system. Documentation and Users Guide.
FAO, 2000. Technical Conversion Factors for Agricultural Commodities. http://www.fao.org/fileadmin/templates/ess/documents/methodology/tcf.pdf.
FAO, 2011. FAOSTAT Online Database. available at link. http://faostat.fao.org/.
Goldstein, A., Fink, L., Meitin, A., Bohadana, S., Lutenberg, O., Ravid, G., 2017. Applying machine learning on sensor data for irrigation recommendations: revealing the agronomist's tacit knowledge. Precis. Agric. 19, 421–444.
Gupta, H.V., Sapriza-Azuri, G., Jódar, J., Carrera, J., 2016. Circulation pattern-based assessment of projected climate change for a catchment in Spain. J. Hydrol. 556, 944–960. https://doi.org/10.1016/j.jhydrol.2016.06.032.
Haylock, M.R., Cawley, G.C., Harpham, C., Wilby, R.L., Goodess, C.M., 2006. Downscaling heavy precipitation over the United Kingdom: a comparison of dynamical and statistical methods and their future scenarios. Int. J. Climatol. 26 (10), 1397–1415.
Koubouris, G.C., Tzortzakis, N., Kourgialas, N.N., Darioti, M., Metzidakis, I., 2015. Growth, photosynthesis and pollen performance in saline water treated olive plants under high temperature. Int. J. Plant Biol. 6. https://doi.org/10.4081/pb(2015.6038).
Kourgialas, N.N., Karatzas, G.P., 2015. A modeling approach for agricultural water management in citrus orchards: cost-effective irrigation scheduling and agrochemical transport simulation. Environ. Monit. Assess. 187, 462. https://doi.org/10.1007/s10661-015-4655-7.
Kourgialas, N.N., Dokou, Z., Karatzas, G.P., 2015. Statistical analysis and ANN modeling for predicting hydrological extremes under climate change scenarios – the example of a small Mediterranean agro-watershed. J. Environ. Manag. 154, 86–101.
Kourgialas, N.N., Koubouris, G.C., Karatzas, G.P., Metzidakis, I., 2016. Assessing water erosion in Mediterranean tree crops using GIS techniques and field measurements: the effect of climate change. Nat. Hazards 83, 65–81.
Kourgialas, N.N., Karatzas, G.P., Koubouris, G.C., 2017. A GIS policy approach for assessing the effect of fertilizers on the quality of drinking and irrigation water and wellhead protection zones (Crete, Greece). J. Environ. Manag. 189, 150–159.
Koutroulis, A.G., Tsanis, I.K., Daliakopoulos, I.N., Jacob, D., 2013. Impact of climate change on water resources status: a case study for Crete Island, Greece. J. Hydrol. 479, 146–158.
Loukas, A., Vasiliades, L., Tzabiras, J., 2008. Climate change effects on drought severity. Adv. Geosci. 17, 23–29.
Mertens, J., Madsen, H., Kristensen, M., Jacques, D., Feyen, J., 2005. Sensitivity of soil parameters in unsaturated zone modelling and the relation between effective, laboratory and in situ estimates. Hydrol. Process. 19, 1611–1633. https://doi.org/10.1002/hyp.5591.
Michelakis, N., Vouyoukalou, E., Clapaki, G., 1996. Water use and soil moisture depletion by olive trees under different irrigation conditions. Agric. Water Manag. 29 (3), 315–325.
Milano, M., Ruelland, D., Fernandez, S., Dezetter, A., Fabre, J., Servat, E., Fritsch, J.M., Ardoin-Bardin, S., Thivet, G., 2013. Current state of Mediterranean water resources and future trends under climatic and anthropogenic changes. Hydrol. Sci. J. 58 (3), 498–518.
Nguyen, T.P.L., Mula, L., Cortignani, R., Seddaiu, G., Dono, G., Virdis, S.G., Pasqui, M., Roggero, P.P., 2016. Perceptions of present and future climate change impacts on water availability for agricultural systems in the Western Mediterranean Region. Water 8, 523. https://doi.org/10.3390/w8110523.
Phogat, V., Skewes, M.A., Cox, J.W., Alam, J., Grigson, G., Šimůnek, J., 2013. Evaluation of water movement and nitrate dynamics in a lysimeter planted with an orange tree. Agric. Water Manag. 127.
River Basin Management Plans – GR13, 2015. River Basin District of Crete (GR13). Available from. http://wfdver.ypeka.gr/en/management-plans-en/approved-management-plans-en/.
Sapriza-Azuri, G., Jódar, J., Navarro, V., Slooten, L.J., Carrera, J., Gupta, H.V., 2015. Impacts of rainfall spatial variability on hydrogeological response. Water Resour. Res. 51 (2), 1300–1314.
Schaap, M.G., Leij, F.J, van Genuchten, M.T., 2001. ROSETTA: A computer program for estimating soil hydraulic parameters with hierarchical pedotransfer functions. J. Hydrol. 251 (3–4), 163–176. https://doi.org/10.1016/S0022-1694(01)00466-8.
Seferou, E., Soupios, P., Kourgialas, N.N., Dokou, Z., Karatzas, G.P., Papadopoulos, N., Candasayar, E., Sarris, A., Sauter, M., 2013. Olive oil mill wastewater transport in unsaturated and saturated laboratory conditions using geophysical techniques and the FEFLOW model. Hydrogeol. J. 21 (6), 1219–1234.
Semenov, M.A., Barrow, E.M., 1997. Use of a stochastic weather generator on the development of climate change scenarios. Clim. Chang. 35 (4), 397–414.
Semenov, M.A., Barrow, E.M., 2002. LARS - WG: A Stochastic Weather Generator for Use in Climate Impact Studies.
Shirgure, P.S., 2013. Research review on irrigation scheduling and water requirement in citrus. Sci. J. Rev. 2 (4), 113–121.
Šimůnek, J., Nimmo, J.R., 2005. Estimating soil hydraulic parameters from transient flow experiments in a centrifuge using parameter optimization technique. Water Resour. Res. 41 (4), W04015.
Tan, Q., Shan Zhang, S., Li, R., 2017. Optimal use of agricultural water and land resources through reconfiguring crop planting structure under socioeconomic and ecological objectives. Water 9 (7), 488. https://doi.org/10.3390/w9070488.
Tebaldi, C., Knutti, R., 2007. The use of the multi-model ensemble in probabilistic climate projections. Phil. Trans. R. Soc. A 365 (1857), 2053–2075.
Tsanis, I.K., Koutroulis, A.G., Daliakopoulos, I.N., Jacob, D., 2011. Severe climate-induced water shortage and extremes in Crete. Clim. Chang. 106 (4), 667–677.
Twarakavi, N.K.C., Šimůnek, J., Schaap, M.G., 2010. Can texture-based classification optimally classify soils with respect to soil hydraulics? Water Resour. Res. 46 (1), W01501. https://doi.org/10.1029/2009WR007939.
Udias, A., Pastori, M., Malago, A., Vigiak, O., Nikolaidis, N.P., Bouraoui, F., 2018. Identifying efficient agricultural irrigation strategies in Crete. Sci. Total Environ. 633, 271–284.
Varis, O., Kajander, T., Lemmela, R., 2004. Climate and water: from climate models to water resources management and vice versa. Clim. Chang. 66 (3), 321–344.
Vasiliades, L., Loukas, A., Patsonas, G., 2009. Evaluation of a statistical downscaling procedure for the estimation of climate change impacts on droughts. Nat. Hazards Earth Syst. Sci. 9 (3), 879–894.
Walkley, A., Black, I.A., 1934. An examination of the Degtjareff method for determining soil organic matter and a proposed modification of the chromic acid titration method. Soil Sci. 37, 29–38.
Xu, C.Y., Widen, E., Halldin, S., 2005. Modelling hydrological consequences of climate change - Progress and challenges. Adv. Atmos. Sci. 22 (6), 789–797.